Force Control of Robot Manipulators

OUSSAMA KHATIB AND JOEL BURDICK

Computer Science Department, Stanford University, Stanford, CA 94305, USA

Abstract. *In this paper we discuss issues related to the description of end-effector tasks that involve constrained motion and active force control and present the "generalized position and force specification matrices." Using this task description tool and the end-effector dynamic model in operational space, a unified approach for the control of manipulator motions and active forces is developed. The recent development of the real-time operational space control system, COSMOS, and its implementation in the NYMPH multiprocessor computer are described. Active force control experiments involving zero force control, impact, sliding, and step response are summarized.*

Keywords. Force Control; Manipulation; Robots; Computer Control.

1. Introduction

Current manipulator technology relies primarily on the concept of position control. The ability to perform complex assemblies in unstructured environments is essential to the future of robot manipulators, and suggests the need for control modalities beyond those associated with position. Force control has emerged as one of the basic means to extend robot capabilities in performing advanced tasks in complex environments. The ability to control end-effector forces is not only capable of improving manipulator performance in most operations, but also allows new types of operations previously impossible with position control alone.

Accommodation [Whitney 1977], joint compliance [Paul and Shimano 1976], active compliance [Salisbury 1980], hybrid position/force control [Craig and Raibert 1979], and operational space control [Khatib and Burdick 1986] are among the various methods that have been proposed for manipulator force control. A review of these and other approaches to force control can be found in [Whitney 1985].

In this paper we present a method for the specification of tasks involving simultaneous control of end-effector positions and forces, and develop the "Generalized Position and Force Specification Matrices," which describe these tasks. The fundamentals of the operational space formulation are reviewed, and the integration of motion and force control using the generalized position and force specification matrices and the end-effector dynamic model is presented. The COSMOS system, a multiprocessor operational space control system for a PUMA 560 manipulator, is described, and experimental results involving zero force control, impact, sliding, and step response are summarized.

2. Task Specification

The end-effector motion and contact forces are among the most important components in the planning, description, and control of assembly operations of robot manipulators. The end-effector configuration is represented by a set of m parameters, $x_1, x_2, \ldots, x_m$, specifying its position and orientation in some reference frame. In free motion operations, the number of *end-effector degrees of freedom*, m_0, is defined [Khatib 1980] as the number of independent parameters required to completely specify, in a frame of reference $\mathcal{R}_0$, its position and orientation. A set of such independent configuration parameters forms a system of *operational coordinates*.

In constrained motion operations, the displacement and rotations of the end-effector are subjected to a set of geometric constraints. These constraints restrict the freedom of motion (displacements and rotations) of the end-effector. From the perspective of end-effector control, two elements of information are required for a complete description of the task. These are the vectors of total force and moment that are to be applied in order to maintain the imposed constraints, and the specification of the end-effector motion degrees of freedom and their directions.

Let $\mathbf{f}_d$ be the vector, in the frame of reference $\mathcal{R}_0(\mathcal{O}, \mathbf{x}_0, \mathbf{y}_0, \mathbf{z}_0)$, of the forces that are to be applied by the end-effector. The positional freedom, if any, of the constrained end-effector will therefore lie in the subspace orthogonal to $\mathbf{f}_d$.

A convenient coordinate frame for the description of tasks involving constrained motion operations is a coordinate frame $\mathcal{R}_f(\mathcal{O}, \mathbf{x}_f, \mathbf{y}_f, \mathbf{z}_f)$ obtained from $\mathcal{R}_0$ by a rotation transformation described by S_f such that $\mathbf{z}_f$ is aligned with f_d, as in Fig. 1.

Let us define, in the coordinate frame $\mathcal{R}_f$, the position specification matrix

$$\Sigma_f = \begin{pmatrix} \sigma_x & 0 & 0 \\ 0 & \sigma_y & 0 \\ 0 & 0 & \sigma_z \end{pmatrix}; \qquad (1)$$

where σ_x, σ_y, and σ_z are binary numbers assigned the value 1 when a free motion is specified along the axes $\mathcal{O}x_f$, $\mathcal{O}y_f$, and $\mathcal{O}z_f$ respectively, and zero otherwise. A non-zero value of σ_z implies a full freedom of the end-effector position. In the case of unconstrained end-effector position, the coordinate frame $\mathcal{R}_f$ is assumed to be identical to $\mathcal{R}_0$, and the matrix S_f is the identity matrix.

The directions of force control are described by the force specification matrix $\overline{\Sigma}_f$ associated with Σ_f and defined by

$$\overline{\Sigma}_f = I - \Sigma_f; \tag{2}$$

where I designates the 3×3 identity matrix.

Let us now consider the case where the end-effector task involves constrained rotations and applied moments. Let τ_d be the vector, in the frame of reference $\mathcal{R}_0(\mathcal{O}, x_0, y_0, z_0)$, of moments that are to be applied by the end-effector, and $\mathcal{R}_\tau(\mathcal{O}, x_\tau, y_\tau, z_\tau)$ be a coordinate frame obtained from $\mathcal{R}_0(\mathcal{O}, x_0, y_0, z_0)$ by a rotation S_τ that brings z_τ into alignment with the moment vector τ_d. In $\mathcal{R}_\tau$, the rotation freedom of the end-effector lies in the subspace spanned by $\{x_\tau, y_\tau\}$. To a task specified in terms of end-effector rotations and applied moments in the coordinate frame $\mathcal{R}_\tau$, we associate the the rotation and moment specification matrices Σ_τ and $\overline{\Sigma}_\tau$, defined similarly to Σ_f and $\overline{\Sigma}_f$.

For general tasks that involve end-effector motion (both position and orientation) and contact forces (forces and moments) described in the frame of reference $\mathcal{R}_0$, we define *the generalized task specification matrices*

$$\Omega = \begin{pmatrix} S_f^T \Sigma_f S_f & 0 \\ 0 & S_\tau^T \Sigma_\tau S_\tau \end{pmatrix}; \tag{3}$$

and

$$\widetilde{\Omega} = \begin{pmatrix} S_f^T \overline{\Sigma}_f S_f & 0 \\ 0 & S_\tau^T \overline{\Sigma}_\tau S_\tau \end{pmatrix}; \tag{4}$$

associated with specifications of motion and contact forces, respectively.

The construction of the generalized task specification matrices is motivated by the aim of formulating the selection process in the same coordinate frame (reference frame $\mathcal{R}_0$) where the manipulator geometric, kinematic and dynamic models are formulated. This allows a more efficient implementation of the control system for real-time operations. The task specification matrices, Ω and $\widetilde{\Omega}$, can be constant, configuration-varying, or time-varying matrices. Non-constant generalized task specification matrices correspond to specifications that involve changes in the direction of the applied force vector and/or moment vector, *e.g.* moving the end-effector while maintaining a normal force to a non-planar surface.

3. End-Effector Equations of Motion

Joint space dynamic models, which establish the equations of manipulator joint motions, provide means for the analysis and control of these motions, and for the description of the configuration dependency and interactive nature of these mechanisms. However, the control of end-effector motion and contact forces, or the analysis and characterization of end-effector dynamic performance requires the construction of the model describing the dynamic behavior of this specific part of the manipulator system.

The end-effector motion is the result of those combined joint forces that are able to act along or about the axes of displacement or rotation of the end-effector. These are, indeed, the forces associated with the system of operational coordinates selected to describe the position and orientation of the end-effector. The construction of the end-effector dynamic model is achieved by expressing the relationships between its operational positions, velocities, accelerations, and the virtual operational forces acting on it.

For a non-redundant manipulator, the independent parameters $x_1, x_2, \ldots, x_m$ form a complete set of configuration parameters in a domain of the operational space [Khatib 1980] and thus constitute a system of generalized coordinates. The end-effector equations of motion in operational space can be written as [Khatib 1980, Khatib 1983]

$$\Lambda(\mathbf{x})\ddot{\mathbf{x}} + \mu(\mathbf{x}, \dot{\mathbf{x}}) + \mathbf{p}(\mathbf{x}) = \mathbf{F}; \tag{5}$$

where $\Lambda(\mathbf{x})$ designates the kinetic energy matrix, and $\mu(\mathbf{x}, \dot{\mathbf{x}})$ represents the vector of end-effector centrifugal and Coriolis forces. $\mathbf{p}(\mathbf{x})$ and $\mathbf{F}$ are respectively the gravity and the generalized operational force vectors. With $\mathbf{q}$ representing the vector of n joint coordinates and $J(\mathbf{q})$ the Jacobian matrix, the relationship between $\mathbf{F}$ and the generalized joint forces $\mathbf{\Gamma}$ is given by

$$\mathbf{\Gamma} = J^T(\mathbf{q})\ \mathbf{F}. \tag{6}$$

The control of a manipulator in operational space is based on the selection of the generalized operational forces $\mathbf{F}$ as a command vector. These forces are produced by submitting the manipulator to the corresponding joint forces $\mathbf{\Gamma}$ obtained from equation (6).

As with joint space control systems, the control in operational space can be developed using a variety of control techniques. In operational space control systems, however, errors, performance, dynamics, simplifications, characterizations, and controlled variables are directly related to manipulator tasks. One of the most effective techniques for dealing with these highly nonlinear and strongly coupled systems is *the nonlinear dynamic decoupling approach* [Freund 1975, Zabala Iturralde 1978], which fully exploits the knowledge of the dynamic model structure and parameters. Within this framework of control and at the level of the uncoupled system, linear, nonlinear, robust [Slotine and Khatib 1986], and adaptive [Craig, Hsu, and Shankar Sastry 1986] control structures can be implemented.

Nonlinear dynamic decoupling in operational space is obtained by the selection of the following control structure,

$$\mathbf{F} = \mathbf{F}_m + \mathbf{F}_{ccg}; \tag{7}$$

with:

$$\mathbf{F}_m = \widehat{\Lambda}(\mathbf{x})\mathbf{F}_m^*; \qquad \mathbf{F}_{ccg} = \widehat{\mu}(\mathbf{x}, \dot{\mathbf{x}}) + \widehat{\mathbf{p}}(\mathbf{x}); \tag{8}$$

where, $\widehat{\Lambda}(\mathbf{x})$, $\widehat{\mu}(\mathbf{x}, \dot{\mathbf{x}})$, and $\widehat{\mathbf{p}}(\mathbf{x})$ represent the estimates of $\Lambda(\mathbf{x})$, $\mu(\mathbf{x}, \dot{\mathbf{x}})$, and $\mathbf{p}(\mathbf{x})$. $\mathbf{F}_m^*$ is the command vector of the decoupled end-effector. With a perfect nonlinear dynamic decoupling, the end-effector becomes equivalent to a *single unit mass*, I_{m_0}, moving in the m_0-dimensional space. In order to simplify the notations, the symbol $\widehat{\ }$ will be dropped in the following development.

At the level of the decoupled end-effector, F_m^*, various control structures can be selected. For tasks where the desired motion of the end-effector is specified, a linear dynamic behavior can be obtained by selecting

$$\mathbf{F}^*_m = I_{m_0}\ddot{\mathbf{x}}_d - k_p(\mathbf{x} - \mathbf{x}_d) - k_v(\dot{\mathbf{x}} - \dot{\mathbf{x}}_d); \quad (9)$$

where $\mathbf{x}_d$, $\dot{\mathbf{x}}_d$ and $\ddot{\mathbf{x}}_d$ are the desired position, velocity and acceleration, respectively, of the end-effector. I_{m_0} is the $m_0 \times m_0$ identity matrix. k_p and k_v are the position and velocity gain matrices.

Using equation (6), the joint forces corresponding to the operational command vector $\mathbf{F}$ in (7) can be written as

$$\Gamma = J^T(\mathbf{q})\Lambda(\mathbf{q})\mathbf{F}^*_m + \widetilde{\mathbf{b}}(\mathbf{q}, \dot{\mathbf{q}}) + \mathbf{g}(\mathbf{q}); \quad (10)$$

where $\widetilde{\mathbf{b}}(\mathbf{q}, \dot{\mathbf{q}})$ is the vector of joint forces under the mapping into joint space of the end-effector Coriolis and centrifugal force vector $\mu(\mathbf{x}, \dot{\mathbf{x}})$. A useful form of $\widetilde{\mathbf{b}}(\mathbf{q}, \dot{\mathbf{q}})$ for real-time control and dynamic analysis is [Khatib 1983]:

$$\widetilde{\mathbf{b}}(\mathbf{q}, \dot{\mathbf{q}}) = \widetilde{B}(\mathbf{q})[\dot{\mathbf{q}}\dot{\mathbf{q}}] + \widetilde{C}(\mathbf{q})[\dot{\mathbf{q}}^2]; \quad (11)$$

where $\widetilde{B}(\mathbf{q})$ and $\widetilde{C}(\mathbf{q})$ are the $n \times n(n-1)/2$ and $n \times n$ matrices of the joint forces under the mapping into joint space of the end-effector Coriolis and centrifugal forces.

With the relation (11), the dynamic decoupling of the end-effector can be obtained using the configuration dependent dynamic coefficients $\Lambda(\mathbf{q})$, $\widetilde{B}(\mathbf{q})$, $\widetilde{C}(\mathbf{q})$ and $\mathbf{g}(\mathbf{q})$. By isolating these coefficients, end-effector dynamic decoupling and control can be achieved in a two-level control system architecture. The real-time computation of these coefficients can then be paced by the rate of configuration changes, which is much lower than that of the mechanism dynamics.

4. Constrained Motion Operations

The matrix Ω, defined above, specifies, with respect to the frame of reference $\mathcal{R}_0$, the directions of motion (displacement and rotations) of the end-effector. Forces and moments are to be applied in or about directions that are orthogonal to these motion directions. These are specified by the matrix $\widetilde{\Omega}$.

An important issue related to the specification of axes of rotation and applied moments is concerned with the compatibility between these specifications and the type of representation used for the description of the end-effector orientation. In fact, the specification of axes of rotations and applied moments in the matrices Σ_r and $\overline{\Sigma}_r$ are only compatible with descriptions of the orientation using instantaneous angular rotations. However, instantaneous angular rotations are not quantities that can be used as a set of configuration parameters for the orientation. Representations of the end-effector orientation such as Euler angles, direction cosines, or Euler parameters, are indeed incompatible with specifications provided by Σ_r and $\overline{\Sigma}_r$.

Instantaneous angular rotations have been used for the description of orientation error of the end-effector. An angular rotation error vector $\delta\phi$ that corresponds to the error between the actual orientation of the end-effector and its desired orientation can be formed from the orientation description given by the selected representation [Luh, Walker, and Paul 1980, Khatib 1980].

The time-derivatives of the parameters corresponding to a representation of the orientation are related simply to the angular velocity vector. With linear and angular velocities is associated the matrix $J_0(\mathbf{q})$, termed *the basic Jacobian*, defined independently of the particular set of parameters used to describe the end-effector configuration

$$\begin{pmatrix} v \\ \omega \end{pmatrix} = J_0(\mathbf{q})\dot{\mathbf{q}}. \quad (12)$$

The Jacobian matrix $J(\mathbf{q})$ associated with a given representation of the end-effector orientation x_r can then be expressed in the form [Khatib 1980]

$$J(\mathbf{q}) = E_{x_r} J_0(\mathbf{q}); \quad (13)$$

where the matrix E_{x_r} is simply given as a function of x_r.

For end-effector motions specified in terms of Cartesian coordinates and instantaneous angular rotations, the dynamic decoupling and motion control of the end-effector can be achieved [Khatib 1980] by

$$\Gamma = J_0^T(\mathbf{q})\Lambda_0(\mathbf{x})\mathbf{F}^*_m + \widetilde{\mathbf{b}}_0(\mathbf{q}, \dot{\mathbf{q}}) + \mathbf{g}(\mathbf{q}); \quad (14)$$

where $\Lambda_0(\mathbf{q})$ and $\widetilde{\mathbf{b}}_0(\mathbf{q}, \dot{\mathbf{q}})$ are defined similarly to $\Lambda(\mathbf{q})$ and $\widetilde{\mathbf{b}}(\mathbf{q}, \dot{\mathbf{q}})$ with $J(\mathbf{q})$ being replaced by $J_0(\mathbf{q})$.

Using the relationship (13), similar control structures can be designed to achieve dynamic decoupling and motion control with respect to descriptions using other representations for the orientation of the end-effector.

The unified operational command vector for end-effector dynamic decoupling, motion, and active force control can be written as

$$\mathbf{F} = \mathbf{F_m} + \mathbf{F_a} + \mathbf{F_{ccg}}; \quad (15)$$

where $\mathbf{F}_m$, $\mathbf{F}_a$, and $\mathbf{F}_{ccg}$ are the operational command vectors of motion, active force control, and centrifugal, Coriolis, and gravity forces given by

$$\begin{aligned} \mathbf{F}_m &= \Lambda_0(\mathbf{q})\Omega\mathbf{F}^*_m; \\ \mathbf{F}_a &= \widetilde{\Omega}\mathbf{F}^*_a + \Lambda_0(\mathbf{q})\widetilde{\Omega}\mathbf{F}^*_s; \\ \mathbf{F}_{ccg} &= \widetilde{\mathbf{b}}_0(\mathbf{q}, \dot{\mathbf{q}}) + \mathbf{g}(\mathbf{q}); \end{aligned} \quad (16)$$

where $\mathbf{F}^*_s$ represents the vector of end-effector velocity damping that acts in the direction of force control. The joint force vector corresponding to $\mathbf{F}$ in (16), is

$$\begin{aligned} \Gamma = J_0^T(\mathbf{q})[\Lambda_0(\mathbf{q})(\Omega\mathbf{F}^*_m + \widetilde{\Omega}\mathbf{F}^*_s) + \widetilde{\Omega}\mathbf{F}^*_a] \\ + \widetilde{\mathbf{b}}_0(\mathbf{q}, \dot{\mathbf{q}}) + \mathbf{g}(\mathbf{q}). \end{aligned} \quad (17)$$

The control system architecture is shown in Fig. 2, where k_f represents the force error gain and k_{vf} denotes the velocity gain in $\mathbf{F}^*_s$. An effective strategy for the control of the end-effector during the transition from free to constrained motions is based on a pure dissipation of the energy at the impact. The operational command vector $\mathbf{F}_a$ during the *impact transition control* stage is

$$\mathbf{F}_a = \Lambda_0(\mathbf{q})\widetilde{\Omega}\mathbf{F}^*_s. \quad (18)$$

The duration of the impact transition control is a function of the impact velocity and the limitations on damping gains and actuator torques (this duration is typically in the order of tens of milliseconds). Force rate feedback has also been used in $\mathbf{F}^*_s$.

5. COSMOS System

This approach to manipulator force control has been implemented in an experimental manipulator programming and control system, COSMOS. COSMOS is currently implemented in the NYMPH multiprocessor system developed at Stanford [Chen et. al. 1986]. The NYMPH system consists of eight National Semiconductor 32016 microprocessors and a SUN Microsystems workstation integrated on an Intel multibus. The 32016 processors perform the real time computations, while the SUN, via the V-kernel operating system, performs user and system interface functions.

For real time control implementation, the computations of the operational space control can be conveniently decomposed into "high" and "low" and level systems, which can be implemented on parallel processors. The high level system computes the configuration dependent matrices of the dynamic model, while the low level system performs sensor processing and servo computations. Because of the decoupling nature of the control, each of these levels can be furthered divided to extract more parallelism. In the current three processor COSMOS implementation the low level system is divided so that the servos governing the position and orientation degrees of freedom are computed on separate processors.

The orientation kinematics and both position and orientation dynamics, and the run time program decoding functions are implemented in the third processor. With this arrangement, low level servo rates of 200Hz and high level dynamics rates of 100 Hz have been achieved. The architecture of the COSMOS system is shown in Fig. 3.

6. Application

COSMOS has been used for motion and force control of a PUMA 560 manipulator. Generic operations of contact, sliding, and insertion have been demonstrated using this system. Both a force wrist (Stanford/Schieneman design) and the Stanford finger force sensors have been used to provide end-effector force feedback. Finger force sensors provide more accurate and direct measurements of end-effector contact forces. The Stanford finger force sensor is shown in Fig. 4. This sensor consists of three mechanically decoupled flexible load cells to measure the components of forces applied at the finger tip. The inherent flexibility of force sensors must be considered in the design of the force compensator.

With the finger force sensor, the dynamic behavior of the decoupled end-effector/sensor system, in a given direction $\mathbf{z}_f$, can be approximately modeled as a mass and spring oscillator (see Fig. 5). By an appropriate selection of the coordinate origin, the equation of motion along the $\mathbf{z}_f$ direction is

$$m_{z_f}\ddot{z}_f + k_{z_f}z_f = f_{z_a}; \tag{19}$$

where m_{z_f} is the equivalent mass of the manipulator in the z_f direction (m_{z_f} will vary with configuration), k_{z_f} is the equivalent stiffness, and f_{z_a} is the operational force. m_{z_f} and k_{z_f} can be computed as:

$$\begin{aligned} m_{z_f} &= \mathbf{u}^T\Lambda(\mathbf{q})\mathbf{u}; \\ k_{z_f} &= (1/k_s + 1/k_e)^{-1}; \end{aligned} \tag{20}$$

where k_s is the effective stiffnesses of the force sensor, k_e is the effective stiffness of the environment in the $\mathbf{z}_f$ direction, and $\mathbf{u} = [\mathbf{z}_f^T\ 0]^T$.

Based on this simplified model, force control along the z_f direction can be achieved with the control structure

$$f_{z_a} = f_{z_d} + k_f(f_{z_d} - f_z) - m_{z_f}k_{v_f}\dot{z}_f; \tag{21}$$

where f_{z_d} is the desired applied force, and k_f and k_{v_f} are the force error and velocity damping gains. In this simplified model, velocity damping can also be achieved by force derivative feedback, since velocity is proportional to force derivative ($\dot{f}_z = k_{z_f}\dot{z}_f$).

The corresponding operational space command vector for the control of active forces is

$$\mathbf{F}_a = \tilde{\Omega}(\mathbf{F}_d + K_f(\mathbf{F}_d - \mathbf{F}_s)) - K_{v_f}\Lambda\tilde{\Omega}\dot{\mathbf{x}} \tag{22}$$

where K_f and K_{v_f} are diagonal matrices with components k_f and k_{v_f}.

Experiments involving "zero" force control, sliding, impact, step response, and the control of end-effector forces in arbitrary task frames were conducted using the finger force sensors and a PUMA 560 manipulator. In the "zero" force control experiment, the end-effector force is commanded to be zero in one direction, while position and orientation are controlled in the orthogonal directions, so that the end-effector complies with the task. A minimum of 2.5 ounces of forces was required to initiate motion of the end-effector in the force controlled direction. This minimum force is largely due to the effects of joint stiction. In the impact experiments, by using the transition control scheme of equation (18), end-effector bounce was eliminated for impact velocities up to 4.0 in/sec. In the step response experiments, a rise time of 18 milliseconds, and a steady state error of 2.4 ounces was achieved in response to a square wave force command [Khatib and Burdick 1986]. This steady state error can be also be attributed in part to joint stiction effects.

7. Summary and Discussion

In this paper we have presented a useful framework for the integration of motion and force control in manipulators and for the specification of constrained motion tasks. This framework allows a variety of different control techniques to be used within the non-linear decoupling framework.

In the example of section 6 a simple mass/spring model has been used in formulating the active force control command vector at the level of the decoupled end-effector. However, these simple models are only an approximation to the real behavior of manipulators during force controlled operation. Flexibilities and nonlinearities in the manipulator links, joint actuator systems, end-effector gripping devices, and force sensors will contribute additional flexibility and resonant modes to the system. These unmodelled modes limit the level of performance that can be obtained with a control system based on simplified modelling, and thus more complicated control laws that account for the complex and coupled flexibilities in real manipulators need to be considered. In addition, even under the simple mass/spring modeling of section 6, the effective stiffness will change for every different surface with which the manipulator makes contact. Thus, force compensators that are robust in the presence of large variation of effective stiffness are also required.

This approach to motion and force control is based on the precise control of joint torques. However, for most industrial manipulators, such as the PUMA 560, the control of joint torques is difficult to achieve due to gear cogging, friction, stiction, and backlash in the actuator transmission mechanisms. Typically, the actuators of the PUMA used in these experiments exhibit a static dead band that can be as high as 20% of their maximum torque output. The performance achieved in the experimental results has been obtained despite these limitations. These limitations can be minimized by the use of joint torque feedback compensation using joint torque sensing [Luh, Fisher, and Paul 1981], [Pfeffer, Khatib, and Hake 1986], high performance force control ultimately requires both end-effector force sensing and joint torque sensing and control.

Acknowledgements

The authors would like to thank Brian Armstrong and Ron Fearing for their technical assistance. Support for this work has been provided by the National Science Foundation under contract MEA80-19628, by a grant from the Systems Development Foundation, and by DARPA through the Intelligent Task Automation Project, contract F 33615-82-C-5092.

References

Chen, B., Fearing, R., Armstrong, B., and Burdick, J. (1986). Nymph: A Multiprocessor for Manipulation Applications. Proceedings of the 1986 IEEE International Conference on Robotics and Automation, April 7-11, 1986, San Francisco, CA, pp. 1731-1736.

Craig, J.J., Hsu, P., and Shankar Sastry, S. (1986). Adaptive Control of Mechanical Manipulators. Proceedings of the 1986 IEEE International Conference in Robotics and Automation, April 7-11, 1986, San Francisco, pp. 190-195.

Craig, J.J. and Raibert, M. (1979). A Systematic Method for Hybrid Position/Force Control of a Manipulator. Proceedings 1979 IEEE Computer Software Applications Conference, Chicago.

Freund, E. (1975). The Structure of Decoupled Non Linear Systems. *International Journal of Control*, vol. 21, no. 3, pp. 443-450.

Khatib, O. (1980). Commande Dynamique dans l'Espace Opérationnel des Robots Manipulateurs en Présence d'Obstacles. Thése de Docteur-Ingénieur. École Nationale Supérieure de l'Aéronautique et de l'Espace, Toulouse, France.

Khatib, O. (1983). Dynamic Control of Manipulators in Operational Space. Sixth CISM-IFToMM Congress on Theory of Machines and Mechanisms, December 15-20, 1983, pp. 1128-1131, New Delhi, India (Wiley, New Delhi).

Khatib, O. and Burdick, J. (1986). Motion and Force Control of Robot Manipulators. Proceedings of the 1986 IEEE International Conference on Robotics and Automation, April 7-11, 1986, San Francisco, pp. 1381-1386.

Luh, J.Y.S., Fisher, W.D., and Paul, R.P. (1981). Joint Torque Control by a Direct Feedback for Industrial Robot. Proc. 20th IEEE Conference on Decision and Control, December 1981, San Diego, pp. 265-271.

Luh, J.Y.S. Walker, M.W. and Paul, P. (1980). Resolved Acceleration Control of Mechanical Manipulators. IEEE Transactions on Automatic Control, no. 3, pp. 468-474.

Paul, R.P. and Shimano, B. (1976). Compliance and Control. Proceedings of the Joint Automatic Control Conference, July 1976, pp. 694-699. Purdue University.

Pfeffer, L. Khatib, O. and Hake, J. (1986). Joint Torque Sensory Feedback in the Control of a PUMA Manipulator. Proceedings of the 1986 American Control Conference, Seattle.

Salisbury, J.K. (1980) Active Stiffness Control of a Manipulator in Cartesian Coordinates. 19th IEEE Conference on Decision and Control, December 1980, Albuquerque, New Mexico.

Slotine, J.J. and Khatib, O. 1986 (June). Robust Control in Operational Space for Goal Positioned Manipulator Tasks. The 1986 American Control Conference, Seattle.

Whitney, D.E. (1977). Force Feedback Control of Manipulator Fine Motions. ASME, Journal of Dynamic Systems, Measurement, and Control, June 1977, pp. 91-97.

Whitney, D.E. (1985). Historical Perspective and State of the Art in Robot Force Control. Proceedings of the 1985 IEEE International Conference on Robotics and Automation, March 1985, pp. 262-268, St. Louis.

Zabala Iturralde, J. (1978). Commande des Robots Manipulateurs à partir de la Modélisation de leur Dynamique. Thèse de 3ème Cycle, Université of Paul Sabatier, Toulouse, France.

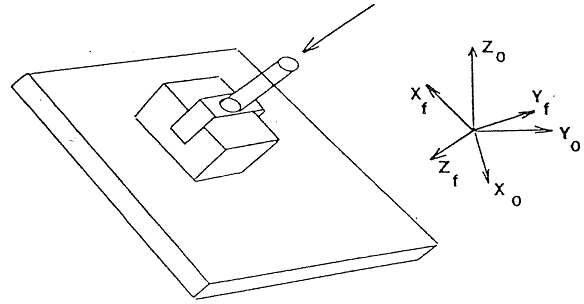

Fig. 1. *Constrained motion task*

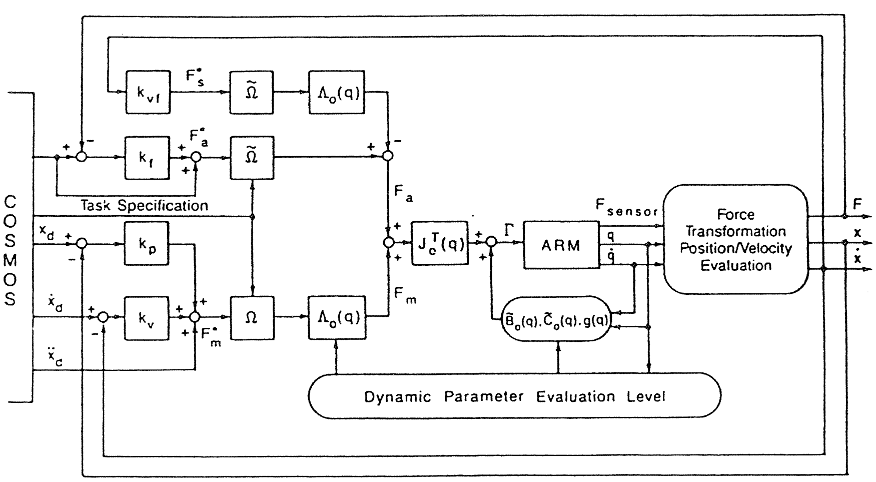

Fig. 2. *Operational Space control system architecture*

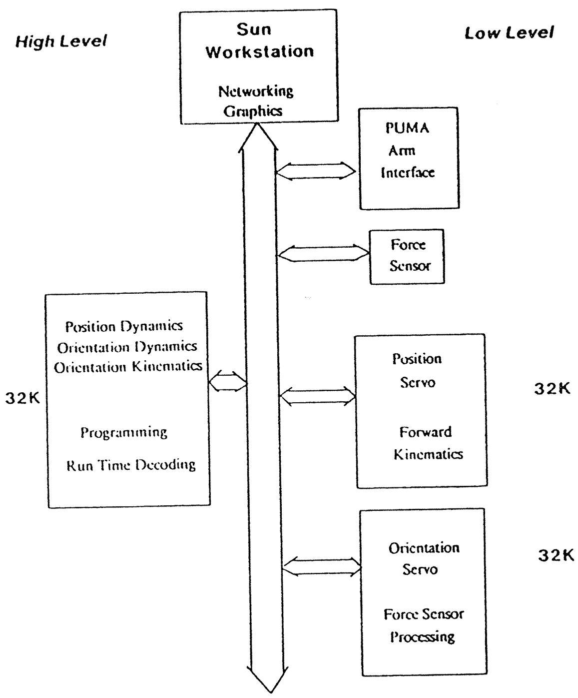

Fig. 3. *COSMOS multiprocessor architecture*

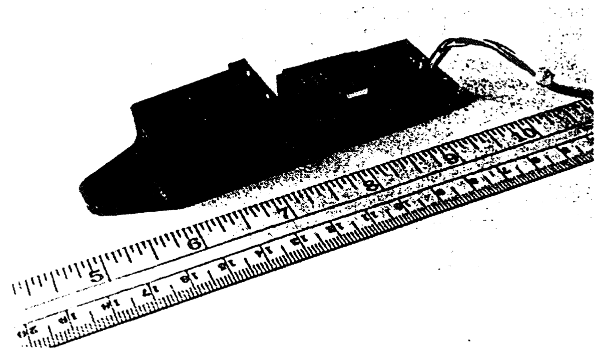

Fig. 4. *Stanford Finger force sensor*

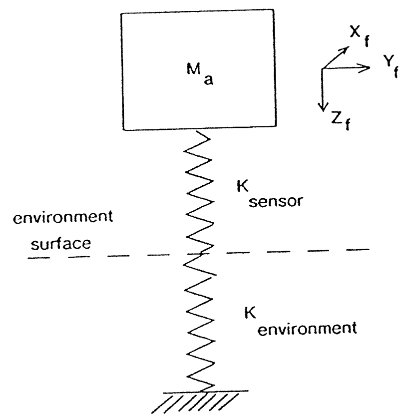

Fig. 5. *Simplified end-effector force sensor model*

RÉSUMÉ

Nous presentons dans cet article une méthode pour le côntrole des forces d'un manipulateur qui est basée sur la modèlisation dynamique dans l'espace opérationnel. Nous spècifions des tâches mettant en jeu à la foi le controle de force et de position en utilisant des "matrices généralisées de position/force." Ces matrices et un modèle dynamique de l'organe terminal forment la base d'une approache intégrée du contrôle de position et de force.